Supplemental Document

Optics EXPRESS

Active control of mid-wavelength infrared non-linearity in silicon photonic crystal slab: supplement

RIHAN WU,[1] MIGUEL NAVARRO-CIA,[1,2] DIMITRI CHEKULAEV,[3] JACK COLLINS,[1] AND ANDREY KAPLAN[1,*]

[1] *School of Physics and Astronomy, University of Birmingham, Birmingham, UK*
[2] *Department of Electronic, Electrical and Systems Engineering, University of Birmingham, Birmingham, UK*
[3] *Department of Chemistry, University of Sheffield, Sheffield S3 7HF, UK*
[*] *a.kaplan.1@bham.ac.uk*

Supplement DOI: https://doi.org/10.6084/m9.figshare.24239029

Parent Article DOI: https://doi.org/10.1364/OE.497371

Active Control of Mid-Wavelength Infrared Non-linearity in Silicon Photonic Crystal Slab: supplemental document

1. CARRIER DENSITY ESTIMATE FOR 50% MODULATION CONTRAST IN SILICON FOR THE WAVELENGTH OF 4 MICRON

A simple estimate can be made using the empirical formula available in the literature for the free carrier absorption coefficient, α_{free}, for infra-red light [1]:

$$\alpha_{free} = 10^{-18} n\lambda,$$

where for the free carrier density, n, of 10^{19} cm^{-3} and $\lambda = 4\mu$m, α_{free} is 160 cm^{-1}. To achieve the transmittance $T = 0.5$, one might assume a slab of the thickness d uniformly ejected with free carriers. Thus, the thickness of the slab is $d = -\frac{ln(T)}{\alpha_{free}} \sim 43\mu$m.

Moreover, it can be further estimated that to achieve the carrier density, n, of 10^{19} cm^{-3}, by optical pumping with wavelength of 800 nm at the near-infrared range, one will need to apply the fluence of a few tens millijoules, while taking into the account that the absorption coefficient for silicon is 827 cm^{-1} [ref.[2]].

2. NUMERICAL CALCULATIONS

A. Band structure

To calculate the band structure of the 2D SiPhC, we employ the finite-difference time-domain package of Ansys Optics (formerly known as Lumerical). Following the standard procedure for non-rectangular lattices, we construct a rectangular FDTD simulation region periodic in x and y directions (1.5 μm and $1.5\sqrt{3}$ lattice constant, respectively) by including multiple unit cells with a hole diameter of 1 μm. The measured complex index of refraction of silicon for pumped and unpumped cases is imported and used for the material definition in each case. A uniform mesh with mesh steps of 20 and 17 nm in the x and y direction, respectively, is used to ensure that the mesh does not break the periodicity of the system. In addition, the software-defined conformal variant 0 mesh refinement type is used. We excite all possible system modes by using eight randomly placed broadband dipoles. The wave vector k is specified by the Bloch boundary conditions, which means one simulation per k-vector is required. The bands (i.e., modes) are identified by finding the resonant frequencies of the fields that persist in the simulation. To this end, the software-defined bandstructure object collects the electric field as a function of time for ten randomly placed time monitors and adds them together. Simulations are terminated when the residual energy in the calculation volume is 10^{-5} of its peak value.

B. Electric field distribution

The frequency domain solver of CST Microwave Studio is used to simulate the response of the 15-μm-thick SiPhC slab with the geometrical dimensions given in the main text; lattice and hole diameters are 1.5 and 1 μm, respectively. The measured complex index of refraction of silicon for pumped and unpumped cases is imported and used for the material definition in each case. The software-defined unit cell boundary condition and the Floquet ports with 6 Floquet modes are used. An adaptive tetrahedral mesh is employed to ensure convergence, resulting in a minimum and maximum tetrahedral edge length of 0.107 and 1.721 μm, respectively, for the pumped case and 0.116 and 1.128 μm, respectively, for the unpumped case. A 10^{-4} linear equation system solver accuracy regarding the relative residual norm is used as the simulation termination criterion. An xy cross-sectional E-field monitor records the field at 4 μm when the incident field is 20°.

3. GUIDED RESONANCES IN SIPHC

A 15x objective was used to loosely focus the IR beam on the sample. The transmitted light was collected by another 15x objective and analysed by a Fourier Transform Infrared Spectrometer equipped with a liquid nitrogen-cooled Mercury-Cadmium-Telluride (MCT) detector. To enhance the coupling of the incoming light to the guided modes, the sample was tilted to the incidence angle of 20°. The incoming light was *p*-polarised, and the sample was oriented to align the $\Gamma - K$ direction along the plane of incidence. The transmittance spectra of the SiPhC and the reference of the uniform silicon slabs are shown in Fig. S1. The spectra mainly consist of periodically spaced Fabry-Pérot fringes for both samples. However, for the SIPhC slab, the periodicity of the fringes is interrupted in the places corresponding to $\omega a/2\pi c$ of $\sim$0.37 and $\sim$0.45, while for the reference, it is equally spaced for the entire spectral range. Referring to Fig. 2 in the main text, these frequencies correspond to the light line crossing the guided TM modes. At these conditions, the external light can be coupled to the modes and confined while propagating along the "veins" of the slab. It can be seen that the transmittance at these frequencies drops below the fringes level, suggesting that there is more absorption of the confined light propagating through the medium than for frequencies where no coupling is expected, and light is delocalised.

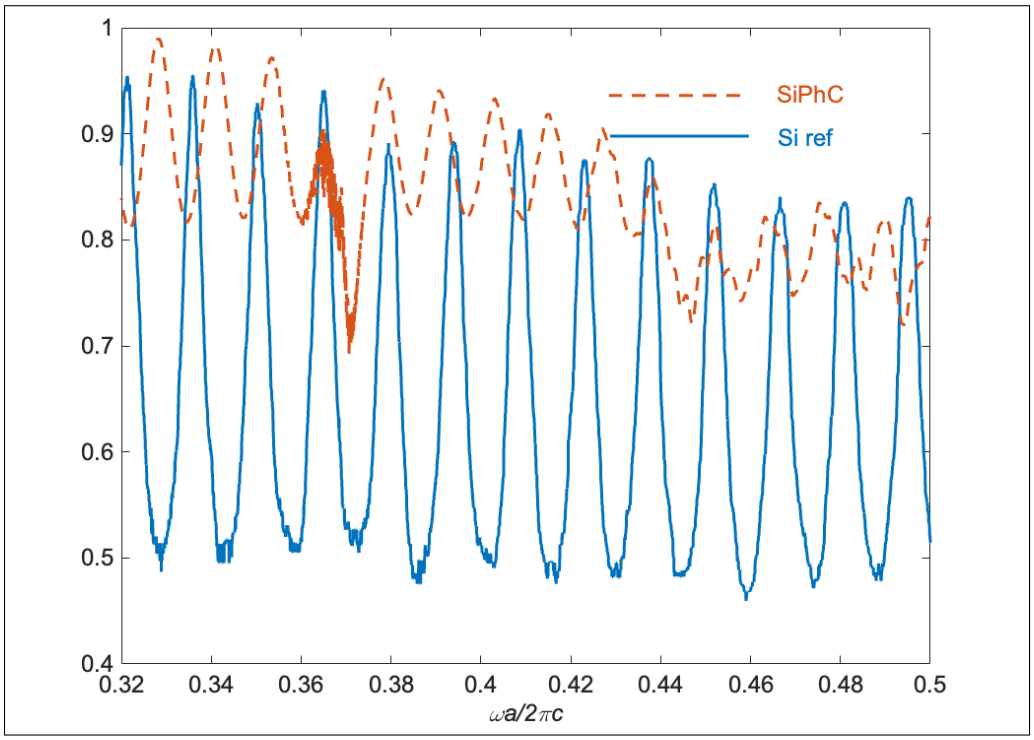

Fig. S1. Infrared transmittance, T, spectra of SiPhC (red dashed line) and silicon slab reference, Si ref, material (blue solid line) as a function of dimensionless parameter $\omega a/2\pi c$.

4. RULING OUT A RESIDUAL HEAT INDUCED BY THE PUMP BEAM AS A FACTOR AFFECTING NON-LINEARITY CHANGE

We performed a series of experiments to confirm that applying the optical pump changes the non-linear response by injecting free carriers and negating the effect of heat produced by pump absorption. Figure S2 (a) shows the Z-scans absorptance measurements of SiPhC and silicon bulk slabs. The measurements were performed by setting the pump arrival time before or after the probe. The red and blue dashed lines show the measurement when the pump arrives after the probe. In this condition, the probe propagation through a sample is not affected by the carriers excited by the pump. However, it could be influenced by residual heat if such accumulates from shot-to-shot pump pulses impinged on the samples. It can be seen that this is not the case, as the Z-scan absorptance remains nearly identical to that recorded without the pump, as shown in

the main text in Fig. 3(a). The solid lines correspond to the setting of the pump's arrival before the probe. Here the excitation of the free carriers occurs before the probe. This excitation is the leading cause of reducing the non-linear absorptance.

Moreover, we investigated the time-resolved response of the non-linear absorptance change ($\Delta A/A_0$) for SiPhC and silicon bulk slabs, shown in Figure S2 (b). The measurements were conducted under two experimental conditions: the probe beam was loosely or tightly focused on the sample. The decay dynamics remain consistent across all cases. This further corroborates the argument in the main text, which suggests that the injected free carriers do not directly contribute to the non-linearity. Instead, their presence alters the crossing point of photonic bands and the light line by modulating the material's refractive index. It is worth noting that the pump-induced thermal effect can also induce changes in the material's refractive index. However, thermal effects are long-lasting phenomena and would persist even before time zero, as preceding pump pulses initiate them. If the non-linear change in absorptance were attributed to the pump-induced thermal effect rather than carrier injection, it would exhibit a constant behaviour before and after time zero. Conversely, Figure 2(b) clearly illustrates that the absorptance varies under different probe focusing conditions after time zero, indicating that the injection of free carriers causes this change.

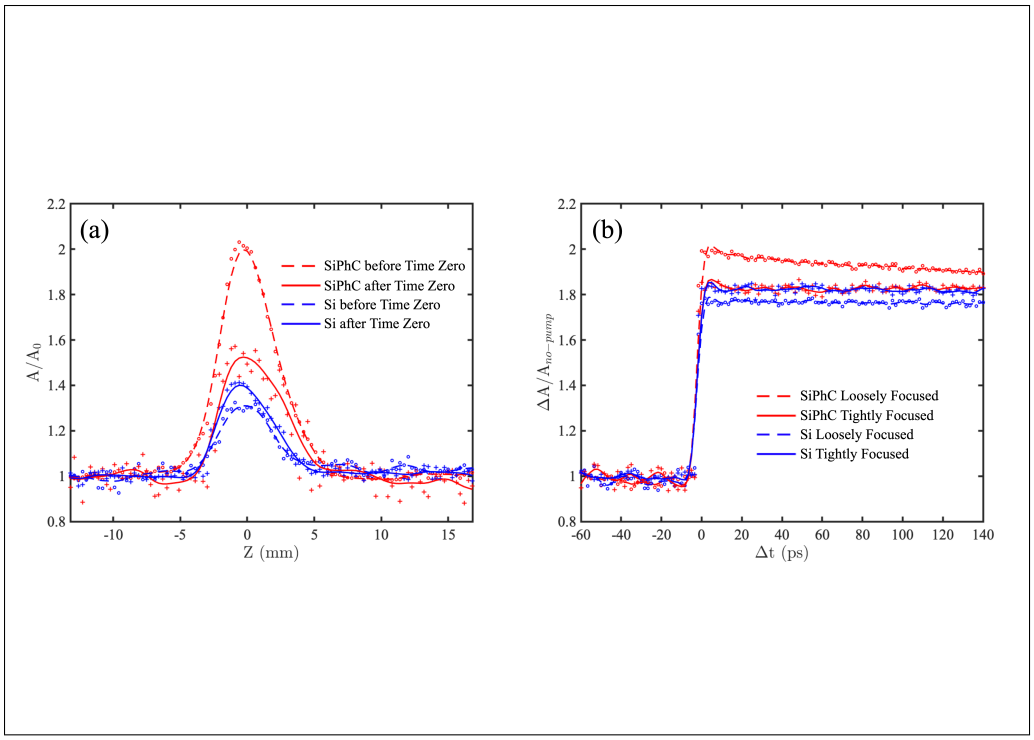

Fig. S2. (a)Z-scan, normalised absorptance, A/A_0, of 4 μm wavelength for the 15-μm-thick uniform silicon (Si ref) and SiPhC slabs, both are 15 μm-thick. Dashed lines represent measurements for the pump beam arriving after the probe. In contrast, the solid lines indicate the reverse arrival timing. (b) Fractional change of the absorptance, $\Delta A/A_{no-pump}$, as a function of the arrival time difference between the pump and probe pulses. The dashed and solid lines represent the loose and tightly focusing of the probe beam, respectively.

REFERENCES

1. D. Schroder, R. Thomas, and J. Swartz, "Free carrier absorption in silicon," IEEE J. Solid-State Circuits **13**, 180–187 (1978).
2. C. Schinke, P. Christian Peest, J. Schmidt, R. Brendel, K. Bothe, M. R. Vogt, I. Kröger, S. Winter, A. Schirmacher, S. Lim, H. T. Nguyen, and D. MacDonald, "Uncertainty analysis for the coefficient of band-to-band absorption of crystalline silicon," AIP Adv. **5**, 067168 (2015).